



# Factors influencing diffusion tensor imaging of knee cartilage in children ages 6–12 years: a prospective study

Yilu Zhang<sup>1</sup> · Zhuo Cheng<sup>1</sup> · Hailun Peng<sup>1</sup> · Wei Ma<sup>2</sup> · Rui Zhang<sup>1</sup> · Junya Ma<sup>1</sup> · Sijie Gao<sup>1</sup> · Wei Li<sup>1</sup> · Ye Xu<sup>1</sup>

Received: 14 January 2024 / Revised: 26 May 2024 / Accepted: 28 May 2024 / Published online: 24 June 2024  
© The Author(s), under exclusive licence to Springer-Verlag GmbH Germany, part of Springer Nature 2024

## Abstract

**Background** Magnetic resonance diffusion tensor imaging (DTI) has recently been used to evaluate the developing cartilage of children, but the influencing factors have not been well studied.

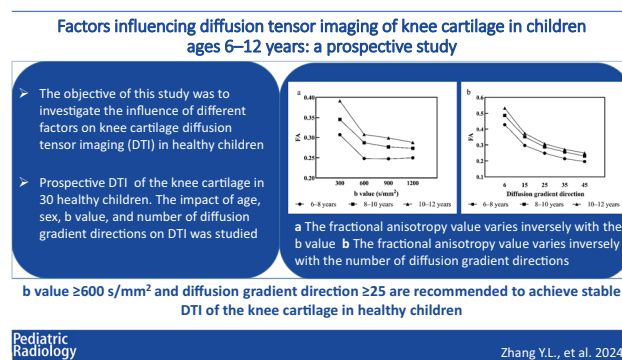
**Objective** The objective of this study was to investigate the influence of the diffusion gradient strength (b value), diffusion gradient direction, age and sex on knee cartilage DTI in healthy children aged 6–12 years.

**Materials and methods** A total of 30 healthy child volunteers, with an average age of  $8.9 \pm 1.6$  (mean  $\pm$  standard deviation) years, were enrolled in this study. They were categorized into three groups according to their age range: 6–8 years, 8–10 years and 10–12 years, ensuring equal sex distribution in each group (5 boys and 5 girls). These volunteers underwent routine left knee joint magnetic resonance imaging (MRI) and serial DTI scans. DTI parameters were altered as follows: when b value =  $600 \text{ s/mm}^2$ , diffusion gradient direction was set to 6, 15, 25, 35 and 45; and when diffusion gradient direction = 25, b value was set to 300, 600, 900 and  $1200 \text{ s/mm}^2$ . The values of fractional anisotropy (FA) and apparent diffusion coefficient (ADC) were separately acquired using image post-processing techniques. The correlation between various b values, diffusion gradient directions, age and sex on the one hand and FA and ADC values on the other, was investigated.

**Results** (1) When diffusion gradient direction was fixed and the b value was varied, both FA and ADC exhibited a decreasing trend as the b value increased ( $P < 0.001$ ). (2) When the b value was fixed and diffusion gradient direction was varied, the FA of knee cartilage showed a decreasing trend with increasing diffusion gradient direction ( $P < 0.001$ ). (3) The FA value increased with age ( $P < 0.05$ ).

**Conclusion** The b value, diffusion gradient direction value and age exert a significant impact on both FA and ADC values in MR DTI of knee cartilage in children aged 6–12 years. In order to obtain a stable DTI, it is recommended to select a b value  $\geq 600 \text{ s/mm}^2$  and a diffusion gradient direction  $\geq 25$  during scanning.

## Graphical Abstract



**Keywords** Cartilage · Children · Diffusion tensor imaging · Knee · Magnetic resonance imaging

Extended author information available on the last page of the article

## Introduction

The growth cartilage and epiphyseal cartilage play crucial roles in children's skeletal development. A variety of acute and chronic disorders can involve cartilage, leading to impaired skeletal development or joint deformity. This primarily occurs due to the lower cell density and limited capacity for self-repair in cartilage, and the damage is typically irreversible [1].

Magnetic resonance imaging (MRI) is currently the sole non-invasive imaging modality for evaluating cartilage damage and repair. MRI techniques, such as delayed gadolinium-enhanced magnetic resonance imaging of cartilage (dGEMRIC), T1 $\rho$  mapping, T2 mapping and diffusion tensor imaging (DTI), have been applied in clinical and experimental studies to assess cartilage. The dGEMRIC technique demonstrates exceptional sensitivity and specificity in quantifying the content of proteoglycans within cartilage. In theory, there is electrostatic repulsion between the negatively charged proteoglycans in cartilage and the anionic contrast agent Gd-DTPA $^{2-}$ . A reduction in proteoglycan concentration leads to increased aggregation of Gd-DTPA $^{2-}$ , resulting in a shorter transverse relaxation time of the cartilage [2]. However, this measurement requires the administration of a double dose of intravenous contrast agent and is primarily used to appraise articular cartilage [3]. The T1 $\rho$  technique can be used for measuring proteoglycan degradation in cartilage. An increase in the T1 $\rho$  value is observed in the presence of alterations in extracellular proteoglycans and collagen fibre density or arrangement compared to that of normal cartilage. However, this measurement relies on long radiofrequency pulses, which may result in an elevation of the specific absorption rate [4]. The transverse magnetization of T2 is predominantly affected by the anisotropy inherent in the structural organization of cartilage tissue, which is intricately linked to the composition, orientation and water content of collagen protein. It provides partial insight into the spatial arrangement of collagen fibres within cartilage; however, its sensitivity and specificity are somewhat constrained [5].

DTI enables non-invasive measurement of water molecule movement in vivo, quantifying water molecules to obtain information on the anisotropy of different tissues, thus studying changes in the microstructure of tissues. If molecules diffuse freely, the MRI signal decreases in all directions, but if diffusion is restricted, it does not [6]. It has been applied in assessing pathologies of the brain and spinal cord, kidney, muscle and peripheral nerves [7, 8]. A growing body of studies also demonstrate its potential in evaluating the organized structure of cartilage, predicting the growth and development of children or assessing

cartilage impairment [9, 10]. DTI has excellent sensitivity for endochondral fibre imaging. The two primary quantitative values obtained from DTI are the fractional anisotropy (FA) and apparent diffusion coefficient (ADC). FA is used to quantify diffusion anisotropy of water molecules within cartilage, which depend on the vectorality of the tissue structure. A FA value close to 0 represents increased diffusion of water molecules in all directions while a FA value close to 1 indicates rich anisotropic structures such as thin fibres. In patients with early cartilage damage, the FA value is significantly lower than in the normal population [11]. ADC reflects the interaction between water molecules and the adjacent environment. An increased ADC value in cartilage often suggests disintegration of the organized and structural extracellular matrix [12]. In short, the accurately measured FA and ADC values are important MRI characteristics of cartilage. However, some previous studies have demonstrated that b value can directly affect the ADC value [13, 14]. We also found in preliminary tests that during DTI scanning of children's cartilage, the selected b value and diffusion gradient direction may produce different FA and ADC values. Similar findings have also been reported in studies on adult and animal cartilage, but the impact of these factors in developing childhood cartilage, to our best knowledge, remains unexplored [15, 16]. Therefore, this study was designed to probe the potential influences on measurement outcomes in DTI scanning of preadolescent and adolescent children's cartilage, aiming to find an optimal combination of b value and diffusion gradient direction.

## Materials and methods

### Subjects

This study was performed in compliance with protocols approved by our institutional research ethics board (protocol number: 2021–222), and informed consent was obtained after the nature of the study had been fully explained.

The study recruited healthy children as volunteers through public advertising between March 2022 and June 2023. The inclusion criteria for subject selection were as follows: (1) age range of 6–12 years; (2) absence of joint swelling, pain, stiffness, restricted movement or deformity upon physical examination; (3) willingness to participate in the study with informed consent/assent provided by both the guardian and the participant. The exclusion criteria were as follows: (1) individuals with claustrophobia or those unable to complete the full examinations for any other reason; (2) individuals suffering from genetic and metabolic disorders, immune system diseases, tumours or other undetermined multisystemic diseases; (3) individuals with a prior history

of trauma, inflammation, infection or surgical intervention on either unilateral or bilateral knee joints; (4) individuals who previously used glucocorticoids, growth hormones, thyroid hormones and other drugs that may impact chondral development; (5) individuals participating in long-term and high-intensity exercise training; (6) volunteers with evident image artefacts that did not have the necessary quality for the study. The inclusion and exclusion process are illustrated in Fig. 1.

### Magnetic resonance imaging and image processing

Before the imaging exam, the volunteers were asked to sit quietly for approximately 5 min to ensure that the left knee remained at rest. MRI of the left knee joint was conducted with a 3-tesla (T) magnetic resonance machine (GE Healthcare, Waukesha, WI) using a dedicated 8-channel knee coil. Both axial T1-weighted imaging (T1W) and DTI data were acquired. The parameters for DTI were as follows: repetition time (TR) = 2035 ms, echo time (TE) = 85 ms, field of view (FOV) = 160 mm × 160 mm, matrix size = 128 × 130, acquired spatial resolution = 1.2 mm × 1.2 mm × 3.0 mm, thickness = 3.0 mm, slices = 16, interslice space = 0 mm, number of excitations = 2. When the b value was set to 600 s/mm<sup>2</sup>, image acquisition was performed separately in a diffusion gradient direction of 6, 15, 25, 35 and 45. When the diffusion gradient direction was fixed at 25, image acquisition was performed separately with b values of 300, 600, 900 and 1200 s/mm<sup>2</sup>. The total scanning time was about 20 mins.

The MR images were transmitted to the GE ADW4.7 (GE Healthcare, Paris, France) working station for further analysis. The DTI software Readyview (GE Healthcare) was employed to automatically generate DTI pseudocolor images, which were carefully selected to showcase the central level of knee joint cartilage, effectively defining its

shape, thickness, and boundary. Four regions of interest (ROIs) within, primarily, epiphyseal cartilage was selected from T1w images and mapped to DTI pseudocolor images (Fig. 2). The regions of interest (ROIs) were placed to maximize inclusion of the cartilage and were drawn using the freehand technique. These regions included the posterior patella, the pre-epiphyseal region of the femoral bone, and the internal and external condyles of the femur. Subsequently, automated calculations generated the corresponding FA and ADC values. The images were measured independently by three certified paediatric radiologists (H.P., W.M. and S.G.) who had at least 5 years of experiences in children's MRI diagnosis and all blinded to the volunteers' personal information. The average FA and ADC values obtained by the three radiologists in all four ROIs were considered representative measurements for the cartilage FA value and ADC value of each volunteer. FA and ADC were calculated using the following formulas:

$$FA = \frac{1}{\sqrt{2}} \sqrt{\frac{(\lambda_1 - \lambda_2)^2 + (\lambda_2 - \lambda_3)^2 + (\lambda_1 - \lambda_3)^2}{\lambda_1^2 + \lambda_2^2 + \lambda_3^2}}$$

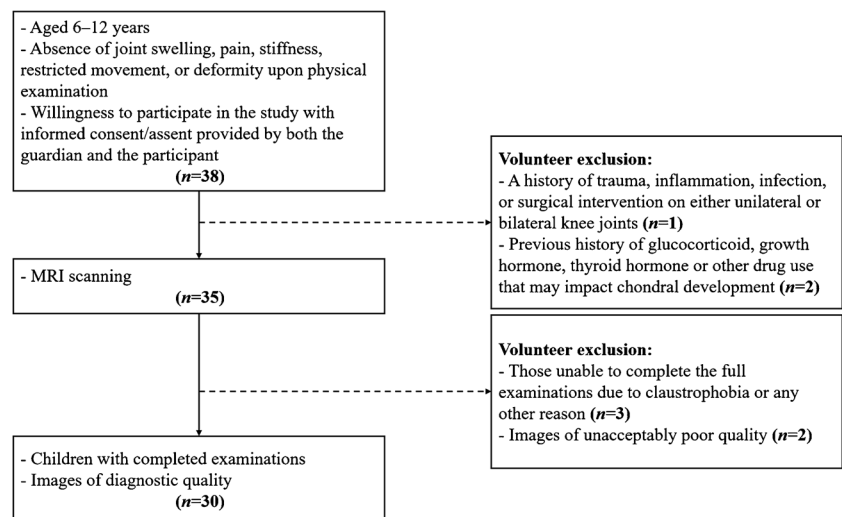
$$ADC = \frac{\lambda_1 + \lambda_2 + \lambda_3}{3}$$

where  $\lambda_1$ ,  $\lambda_2$  and  $\lambda_3$  are three non-zero components (i.e. eigenvalues) [17].

### Statistical analysis

The statistical analysis was conducted using SPSS (Version 19.0, SPSS Inc, Chicago, IL) and GraphPad Prism (Version 9.5, GraphPad Software Inc, San Diego, CA). The intraclass correlation coefficient (ICC) was used to

**Fig. 1** Flowchart of the study population



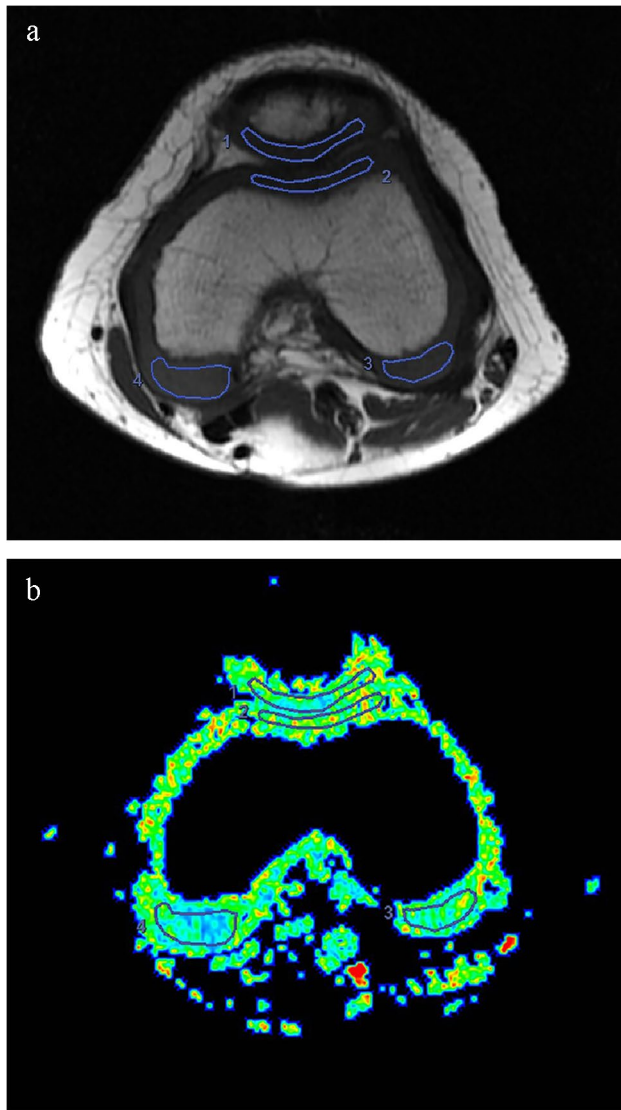


**Fig. 2** A healthy 7-year-old boy. **a** Axial T1W imaging of the left knee joint shows manually delineated regions of interest (ROIs) for cartilage (posterior patella, pre-epiphyseal region of the femoral bone, and internal and external condyles of femur). **b** The ROIs on the T1W imaging are mapped to the image of fractional anisotropy (FA). The colour scale represents the range of FA values (0.00–0.60)

evaluate the consistency of radiologists' measurements. The Kruskal–Wallis rank sum test or Mann–Whitney U test were used when normality and homogeneity of variance assumptions were not satisfied. Spearman's correlation coefficients were calculated to assess the relationships between FA and b values, FA and diffusion gradient direction, FA and age, and FA and sex and the relationships between ADC and b values, ADC and diffusion gradient direction, ADC and age, and ADC and sex. Pearson's correlation techniques were used to probe the relationships between FA and age and between ADC and age.  $P < 0.05$  was considered statistically significant.

## Results

### Subjects and consistency of radiologists' measurements

A total of 30 child volunteers were ultimately enrolled in the study, comprising an equal distribution of 15 boys and 15 girls aged between 6 and 12 years, with an average age of  $8.9 \pm 1.6$  (mean  $\pm$  standard deviation) years. They were categorized into three groups based on age: 6–8 years old, 8–10 years old and 10–12 years old. Each group consisted of five boys and five girls.

The interrater reliability for FA measurement among the three radiologists was excellent, with an ICC of 0.999 ( $P < 0.001$ ), while the interrater reliability for ADC measurement was high, with an ICC of 0.980 ( $P < 0.001$ ).

### Effect of b value on fractional anisotropy and apparent diffusion coefficient

According to the results of the Kruskal–Wallis test, both FA values and ADC values exhibited significant differences among different b values ( $P < 0.001$ ). Dunn's multiple comparisons test showed that only the FA values at b value =  $300 \text{ mm}^2/\text{s}$  differed significantly from those at any other b value ( $P < 0.001$ ); no significant difference was observed between any two of the remaining b values, and there were significant differences in ADC values between each pair of b values ( $300 \text{ s}/\text{mm}^2$  vs.  $600 \text{ s}/\text{mm}^2$  ( $P = 0.0195$ ),  $300 \text{ s}/\text{mm}^2$  vs.  $900 \text{ s}/\text{mm}^2$  ( $P < 0.001$ ),  $300 \text{ s}/\text{mm}^2$  vs.  $1200 \text{ s}/\text{mm}^2$  ( $P < 0.001$ ),  $600 \text{ s}/\text{mm}^2$  vs.  $900 \text{ s}/\text{mm}^2$  ( $P = 0.0222$ ),  $600 \text{ s}/\text{mm}^2$  vs.  $1200 \text{ s}/\text{mm}^2$  ( $P < 0.001$ ),  $900 \text{ s}/\text{mm}^2$  vs.  $1200 \text{ s}/\text{mm}^2$  ( $P = 0.023$ )) (Fig. 3). Furthermore, Spearman's correlation analysis showed a significant negative correlation between b values and FA ( $P < 0.001$ ), as well as between b values and ADC ( $P < 0.001$ ). Additionally, both FA and ADC exhibited a decline with increasing b value (Fig. 4). FA values reached a plateau when the b value was higher than  $600 \text{ s}/\text{mm}^2$  (Fig. 5).

### Effect of diffusion gradient direction on fractional anisotropy and apparent diffusion coefficient

According to the Kruskal–Wallis test, there was a significant difference in FA among different diffusion gradient direction overall ( $P < 0.001$ ), whereas no significant difference was observed for ADC ( $P = 0.995$ ). Dunn's multiple comparisons test of FA values revealed significant differences between some pairs of diffusion gradient direction (6 vs. 15 ( $P = 0.0074$ ), 6 vs. 25 ( $P < 0.001$ ), 6 vs. 35 ( $P < 0.001$ ), 6 vs. 45 ( $P < 0.001$ ),

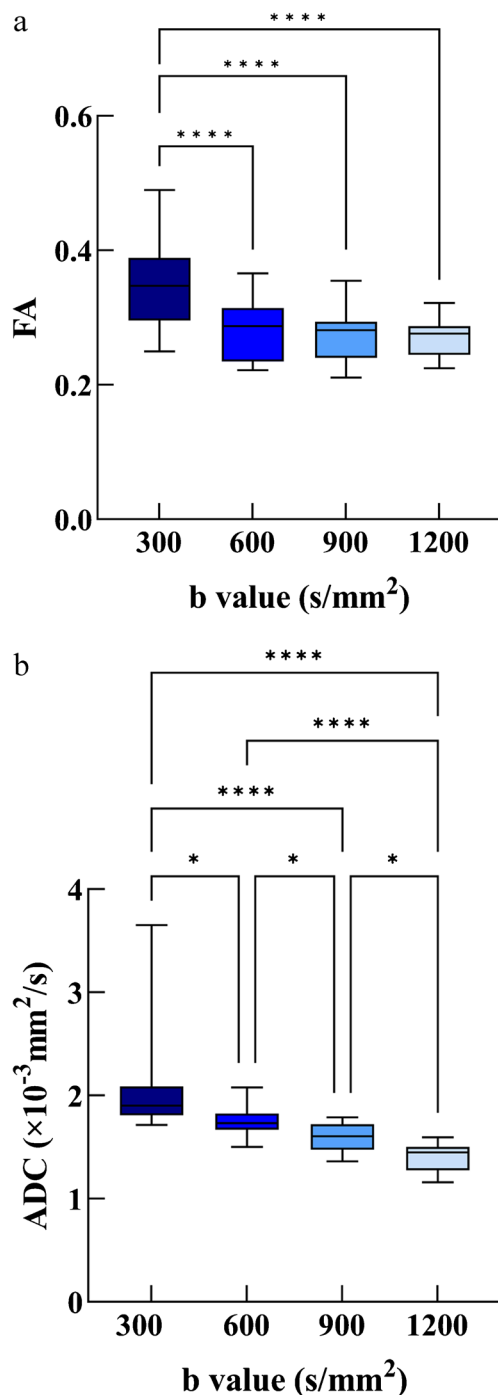


**Fig. 3** **a** Comparison of fractional anisotropy (FA) between any two b values. **b** Comparison of apparent diffusion coefficient between any two b values. *ADC* apparent diffusion coefficient. \* $P < 0.05$ , \*\*\*\* $P < 0.0001$

15 vs. 35 ( $P = 0.0001$ ), 15 vs. 45 ( $P < 0.001$ ), 25 vs. 45 ( $P = 0.0225$ ); no significant differences were found between the following pairs of diffusion gradient direction: 15 vs. 25 ( $P = 0.0956$ ), 25 vs. 35 ( $P = 0.6896$ ), 35 vs. 45 ( $P > 0.9999$ ) (Fig. 6). Furthermore, Spearman's

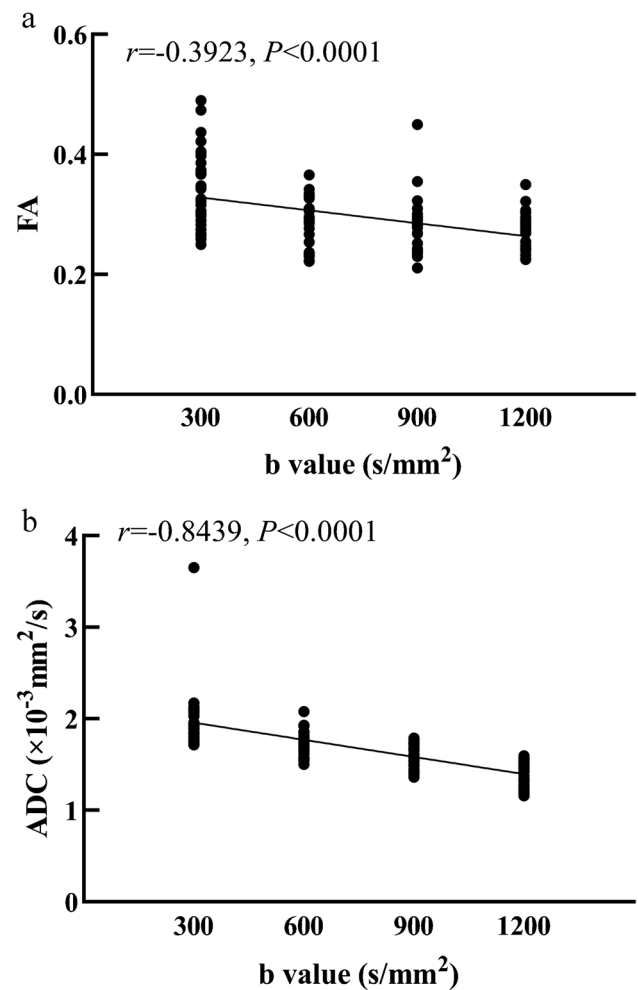


**Fig. 4** **a** The fractional anisotropy (FA) decreased as the b value increased. **b** The apparent diffusion coefficient decreased as the b value increased. *ADC* apparent diffusion coefficient

correlation analysis indicated that as the diffusion gradient direction increased, there was a decrease in FA ( $r = -0.8227$ ,  $P < 0.0001$ ) (Fig. 7). The FA value exhibits a decreasing trend as the diffusion gradient direction increases, and the rate of attenuation slows down when the diffusion gradient direction  $> 25$  (Fig. 5).

### Effect of age and sex on fractional anisotropy

Spearman's correlation analysis showed a significant positive correlation between age and FA ( $P < 0.05$ ). Furthermore, there was an increase in FA with increasing age (Fig. 8).

The Mann–Whitney  $U$  test showed that there was a significant difference in FA values between males and females ( $Z = -3.259$ ,  $P = 0.001$ ), and no significant difference in ADC values between males and females ( $Z = -1.275$ ,  $P = 0.202$ ). Figure 9 shows the variation curve of FA values



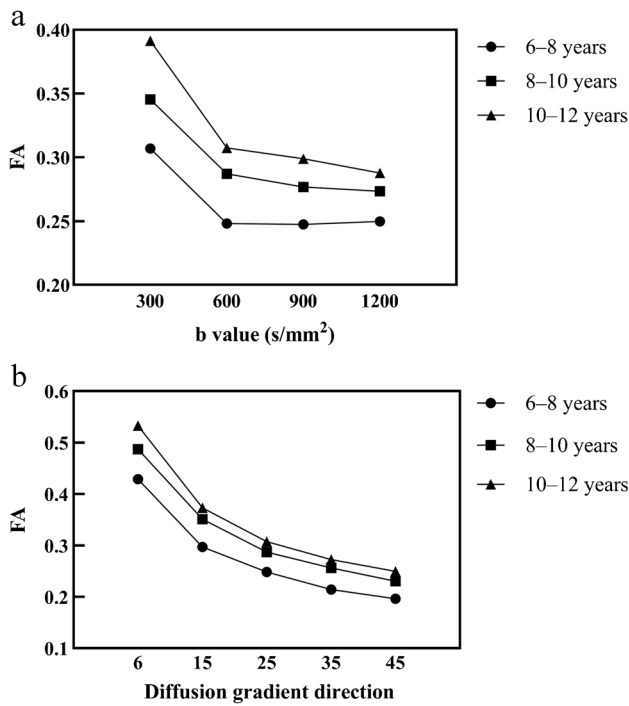


**Fig. 5** **a** The relationship between the fractional anisotropy (FA) and b values for each ages. **b** The relationship between FA and diffusion gradient direction at different ages

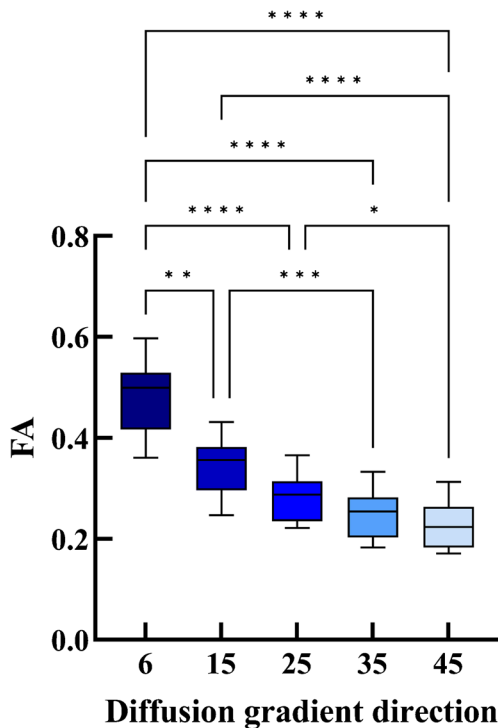


**Fig. 6** Comparison of the value of fractional anisotropy (FA) between any two diffusion gradient directions. \* $P < 0.05$ , \*\* $P < 0.01$ , \*\*\* $P < 0.001$  and \*\*\*\* $P < 0.0001$

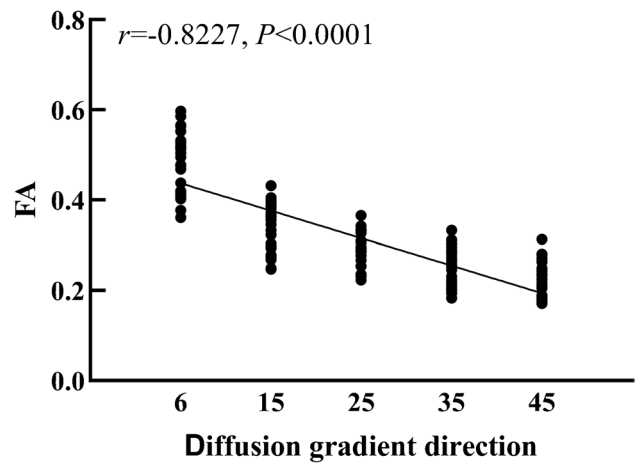


**Fig. 7** Correlation analysis shows that the fractional anisotropy (FA) decreased as the diffusion gradient direction increased

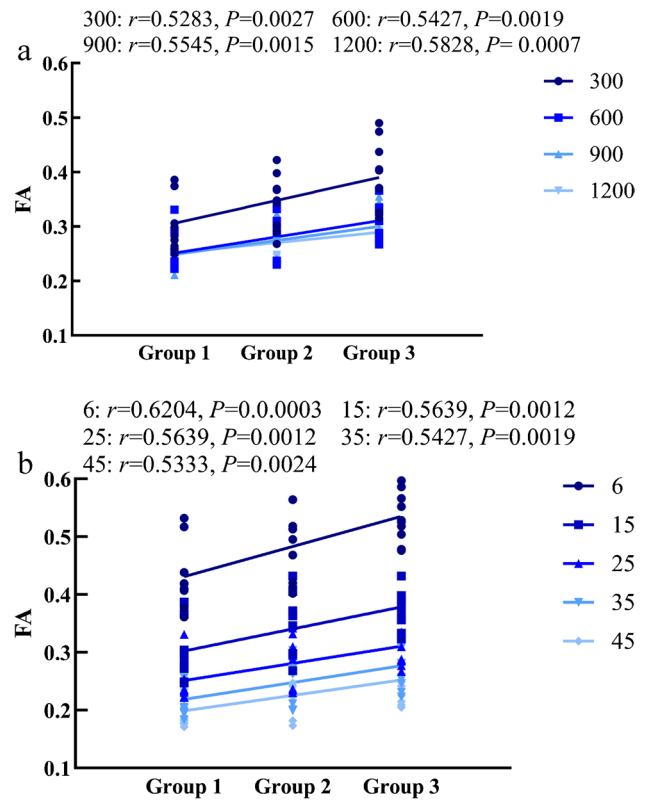


**Fig. 8** **a** A representative plot illustrating the trend of the fractional anisotropy (FA) with age at each given b value (s/mm<sup>2</sup>). **b** Representative plot illustrating the trend of FA with age at each given diffusion gradient directions

for different sexes with the direction of b values or diffusion gradients. It can be seen that the FA value of girls is always higher than that of boys.

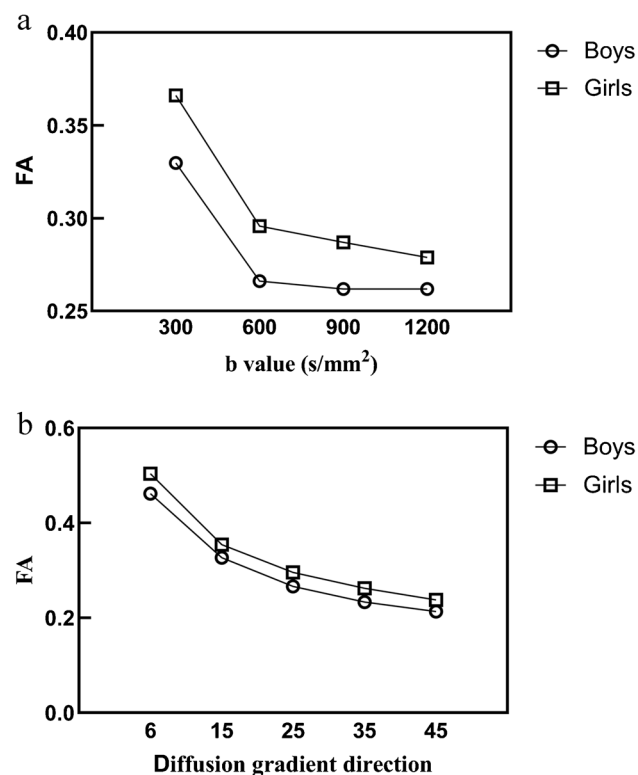


**Fig. 9** a The relationship between the fractional anisotropy (FA) and b values for each sex. b The relationship between FA and diffusion gradient direction for each sex

## Discussion

The epiphyseal cartilage in children undergoes continuous development from the embryonic stage to epiphyseal closure, distinguishing it from adults. The development begins during the 6th week of embryonic life, with joint formation occurring around the 10th week. After birth, the cartilage continues to develop and reaches its maximum thickness at approximately one year of age. The presence of the tide line indicates the completion of cartilage maturation and the termination of intrachondral ossification [18]. The development process is intricately synchronized with the formation of secondary ossification centres, where the developing epiphyseal cartilage undergo progressive maturation over time while simultaneously undergoing structural rearrangement [19]. During different stages of development, there will be corresponding changes in the composition and structure of cartilage. With growth, the collagen fibre structure becomes more organized and stable, leading to a gradual thinning of cartilage, and a decrease in proteoglycan size and accumulation within the matrix [20]. Of interest, multiple studies have demonstrated that among healthy children of similar age groups, girls tend to have smaller joints and thinner cartilage compared to boys [21, 22].

The DTI technique enables quantitative evaluation of the microanatomy, primarily the complex collagen fibre structure, of epiphyseal cartilage, growth plate cartilage and articular cartilage [23]. It can be used for assessing skeletal development in paediatric patients, especially in younger children whose ossific epiphyses have not yet formed or are very small. Moreover, DTI holds potential for investigating the impact of disease on cartilage structure and function, particularly metabolic disorders, immune disorders and chronic arthritis [6, 9]. In clinical settings, DTI technology is predominantly employed for assessing brain microstructure, such as white matter fibre bundle injuries, surgical planning for tumour resection and white matter development. Its application in extracerebral organs including cartilage evaluation remains limited [24–28]. The reasons are not yet fully elucidated. Potential contributing factors may contain challenges in immobilization of extracerebral organs during imaging procedures, insufficiency of directional fibre bundles within these organs, reduced measurement accuracy, a lack of high-quality post-processing algorithm, etc. [29, 30].

In DTI acquisition, the appropriate selection of the number of diffusion gradient directions and b value is crucial. On the one hand, DTI requires an adequate signal-to-noise ratio (SNR) for post-processing while maintaining the desired level of diffusion weighting. In this situation, the b value plays a critical role [31]. A higher b value increase sensitivity to motion diffusion of water molecules and effectively suppresses isotropic diffusion, thereby providing better depict of tissue fibre direction of interest [15]. However, using high b values may lead to issues such as significant tissue signal attenuation and decreased image SNR. Therefore, selecting an optimal b value is essential to obtain high-quality images without compromising SNR. On the other hand, directionality plays a pivotal role in quantifying collagen anisotropy and fibre arrangement. The greater the number of diffusion-sensitive gradients applied in various directions, the higher the directional resolution of DTI, leading to more precise results for fibre bundle tracking. For specific tissues with regular fibre arrangements, a moderate number of diffusion gradient fields applied can adequately reflect the fibre direction. However, excessive application of diffusion sensitivity gradients in multiple directions will unnecessarily prolong scanning time and contribute to potential artifact production [15, 32]. Particularly in knee cartilage DTI scanning, it is necessary to study parameter optimization due to the shorter spin–spin relaxation time and lower water density compared with brain tissue [16].

Many studies have reported the application of DTI in adult articular cartilage, but studies on children's cartilage are relatively few. From the PubMed database, we retrieved only four studies focusing on children's cartilage DTI, with the earliest published in 2017 [9, 33–35]. For DTI studies on adult articular cartilage, a b value of

700–1000 s/mm<sup>2</sup> and a number of diffusion gradient directions greater than 14 has been recommended in the related literature [16, 31]. However, there is limited knowledge regarding the influencing imaging factors and the appropriate DTI parameter settings for the developing cartilage of children. This study attempted to probe these issues and revealed that increasing the b value resulted in a decrease in both FA and ADC measurements and the FA values tended to stabilize when the b value exceeded 600 s/mm<sup>2</sup>. This phenomenon may be attributed to the presence of rich blood vessels in children's cartilage compared to adult cartilage, making measurements at low b values susceptible to microcirculation perfusion and consequently yielding higher FA and ADC values [36]. Therefore, selecting a b value of 600 s/mm<sup>2</sup> is more appropriate due to its ability to maintain stability while avoiding significant decreases in SNR associated with larger b values. This study has also revealed that an increase in the diffusion gradient direction leads to a gradual decrease in FA. This finding highlights the crucial role of the applied diffusion gradient directions in accurately quantifying collagen anisotropy and fibre alignment. The lower number of diffusion gradient directions may induce alterations in each tensor element, ultimately resulting in an overestimation of FA [15]. Notably, FA values tended to be stable in all age groups when the diffusion gradient direction was higher than 25. Therefore, for obtaining consistent results in knee cartilage imaging, it is recommended to use a b value of 600 s/mm<sup>2</sup> and a diffusion gradient direction > 25. These findings align with previous studies by Nian Wang et al. and Qi Zhao et al., although differences could be attributed to variations in magnetic field strength or subject characteristics [15, 16].

In addition, we found a significant positive correlation between FA value and age. The FA value increased with increasing age, which is consistent with the findings reported by Kvist et al. [37]. The fibre orientation and degree of cross-linking in a specific area influence the anisotropic diffusion of cartilage by directing the pore shape through which water diffuses [38]. Changes in collagen structure substantially impact the direction of water molecule dispersion, directly affecting FA values [17, 39]. This may be due to the continuous proliferation of cells in the cartilage as children grow older, resulting in a more orderly arrangement of cells and cell matrix. A more regular tissue structure arrangement will result in stronger diffusion anisotropy of water molecules and a correspondingly higher FA value [40]. Moreover, it has been reported that the SNR of DTI images in older children is diminished, which can potentially result in an overestimation of FA values [34]. In this study, we also observed a higher FA value in girls compared to boys. The reasons for this discrepancy are not fully understood, perhaps it relates to the fact that the female cartilage exhibits thinner dimensions and a greater proportion of transverse

collagen fibres than male cartilage, thereby providing a more complex collagen fibre structure [41].

This study has at least the following limitations. Firstly, due to the potential risks associated with sedation, we did not include children under 6 years old, which may be considered a major limitation. Secondly, the sample size is small and could result in statistical deviations. Thirdly, despite employing multiple radiologists and repeated sampling methods during data processing, manual selection of ROIs may result in errors and biases. Fourthly, the use of T1W imaging to delineate ROIs and maximize the inclusion of cartilage may lead to some articular cartilage being circled into the ROIs. Finally, this study was done with a 3-T MR machine, it is necessary to determine whether the results of this study are applicable to 1.5-T MR scanners. Future studies should aim to include larger sample sizes that encompass children under 6 years old while using more objective automated image processing systems.

In conclusion, the DTI sequence of MRI can be used for quantitative analysis of knee cartilage development in children. It is essential to carefully select appropriate b values and diffusion gradient directions due to their potential influence. To achieve a robust DTI image for children aged 6–12 years, a b value  $\geq 600$  s/mm<sup>2</sup> and diffusion gradient direction  $\geq 25$  may be appropriate.

**Acknowledgements** We sincerely thank Dr. Nie Lisha from GE Healthcare for providing support, which contributed significantly to the success of this research.

**Author contribution** All authors contributed to the study conception and design. Y.X. conceived, supervised and supported the study. Material preparation, data collection and analysis were performed by Y. Z., Z.C., H. P., W.M., S. G. and Y.X. The first draft of the manuscript was written by Y. Z. and all authors commented on previous versions of the manuscript. All authors read and approved the final manuscript.

**Funding** This work was supported by the National Clinical Research Center for child Health and Disorders (grant no.: NCRCCHD-2022-GP-0X) and Chongqing Science and Technology Development Project (grant no.: CSTB2022TIAD-KPX0147).

**Data availability** The datasets generated during and/or analyzed during the current study are available from the corresponding author on reasonable request.

## Declarations

**Conflicts of interest** None

## References

1. Ho-Fung VM, Jaramillo D (2013) Cartilage imaging in children: current indications, magnetic resonance imaging techniques, and imaging findings. *Radiol Clin North Am* 51:689–702. <https://doi.org/10.1016/j.rcl.2013.04.003>



2. Crema MD, Roemer FW, Marra MD et al (2011) Articular cartilage in the knee: current MR imaging techniques and applications in clinical practice and research. *Radiographics* 31:37–61. <https://doi.org/10.1148/rg.311105084>
3. Burstein D, Velyvis J, Scott KT et al (2001) Protocol issues for delayed Gd(DTPA)(2-)-enhanced MRI (dGEMRIC) for clinical evaluation of articular cartilage. *Magn Reson Med* 45:36–41. [https://doi.org/10.1002/1522-2594\(200101\)45:1%3c36::aid-mrm1006%3e3.0.co;2-w](https://doi.org/10.1002/1522-2594(200101)45:1%3c36::aid-mrm1006%3e3.0.co;2-w)
4. Banjar M, Horiuchi S, Gedeon DN, Yoshioka H (2021) Review of quantitative knee articular cartilage MR imaging. *Magn Reson Med Sci* 21:29–40. <https://doi.org/10.2463/mrms.rev.2021-0052>
5. Cheng KY, Lombardi AF, Chang EY, Chung CB (2021) Knee cartilage imaging. *Clin Sports Med* 40:677–692. <https://doi.org/10.1016/j.csm.2021.05.006>
6. Santos LA, Sullivan B, Kvist O et al (2023) Diffusion tensor imaging of the physis: the ABC's. *Pediatr Radiol* 53:2355–2368. <https://doi.org/10.1007/s00247-023-05753-z>
7. Raya JG, Dettmann E, Notohamiprodjo M et al (2014) Feasibility of in vivo diffusion tensor imaging of articular cartilage with coverage of all cartilage regions. *Eur Radiol* 24:1700–1706. <https://doi.org/10.1007/s00330-014-3155-4>
8. Vorona GA, Berman JI (2015) Review of diffusion tensor imaging and its application in children. *Pediatr Radiol* 45(Suppl 3):S375–381. <https://doi.org/10.1007/s00247-015-3277-0>
9. Jaramillo D, Duong P, Nguyen JC et al (2022) Diffusion tensor imaging of the knee to predict childhood growth. *Radiology* 303:655–663. <https://doi.org/10.1148/radiol.210484>
10. Ukai T, Sato M, Yamashita T et al (2015) Diffusion tensor imaging can detect the early stages of cartilage damage: a comparison study. *BMC Musculoskelet Disord* 16:35. <https://doi.org/10.1186/s12891-015-0499-0>
11. Duarte A, Ruiz A, Ferizi U et al (2019) Diffusion tensor imaging of articular cartilage using a navigated radial imaging spin-echo diffusion (RAISED) sequence. *Eur Radiol* 29:2598–2607. <https://doi.org/10.1007/s00330-018-5780-9>
12. Paunipagar BK, Rasalkar D (2014) Imaging of articular cartilage. *Indian J Radiol Imaging* 24:237–248. <https://doi.org/10.4103/0971-3026.137028>
13. Rezaeian A, Ostovari M, Hoseini-Ghahfarokhi M, Khanbabaie H (2022) Diffusion-weighted magnetic resonance imaging at 1.5 T for peripheral zone prostate cancer: the influence of the b-value combination on the diagnostic performance of apparent diffusion coefficient. *Pol J Radiol* 87:e215–e219. <https://doi.org/10.5114/pjr.2022.115715>
14. Maier SE, Wallström J, Langkilde F et al (2022) Prostate cancer diffusion-weighted magnetic resonance imaging: does the choice of diffusion-weighting level matter? *J Magn Reson Imaging* 55:842–853. <https://doi.org/10.1002/jmri.27895>
15. Zhao Q, Ridout RP, Shen J, Wang N (2021) Effects of angular resolution and b value on diffusion tensor imaging in knee joint. *Cartilage* 13:295S–303S. <https://doi.org/10.1177/19476035211007909>
16. Wang N, Mirando AJ, Cofer G et al (2019) Diffusion tractography of the rat knee at microscopic resolution. *Magn Reson Med* 81:3775–3786. <https://doi.org/10.1002/mrm.27652>
17. Agarwal V, Kumar M, Singh JK et al (2009) Diffusion tensor anisotropy magnetic resonance imaging: a new tool to assess synovial inflammation. *Rheumatology (Oxford)* 48:378–382. <https://doi.org/10.1093/rheumatology/ken499>
18. Sophia Fox AJ, Bedi A, Rodeo SA (2009) The basic science of articular cartilage: structure, composition, and function. *Sports Health* 1:461–468. <https://doi.org/10.1177/1941738109350438>
19. Andrade AC, Chrysis D, Audi L, Nilsson O (2011) Methods to study cartilage and bone development. *Endocr Dev* 21:52–66. <https://doi.org/10.1159/000328127>
20. Raya JG, Horng A, Dietrich O et al (2012) Articular cartilage: in vivo diffusion-tensor imaging. *Radiology* 262:550–559. <https://doi.org/10.1148/radiol.11110821>
21. Schneider MT-Y, Rooks N, Besier T (2022) Cartilage thickness and bone shape variations as a function of sex, height, body mass, and age in young adult knees. *Sci Rep* 12:11707. <https://doi.org/10.1038/s41598-022-15585-w>
22. Patel J, Chen S, Katzmeyer T et al (2023) Sex-dependent variation in cartilage adaptation: from degeneration to regeneration. *Biol Sex Differ* 14:17. <https://doi.org/10.1186/s13293-023-00500-3>
23. Van Dyck P, Froeling M, Heusdens CHW et al (2021) Diffusion tensor imaging of the anterior cruciate ligament following primary repair with internal bracing: a longitudinal study. *J Orthop Res* 39:1318–1330. <https://doi.org/10.1002/jor.24684>
24. Perez DL, Nicholson TR, Asadi-Pooya AA et al (2021) Neuroimaging in functional neurological disorder: state of the field and research agenda. *Neuroimage Clin* 30:102623. <https://doi.org/10.1016/j.nicl.2021.102623>
25. Hao X, Liu Z, He S et al (2022) Application of DTI and fMRI in moyamoya disease. *Front Neurol* 13:948830. <https://doi.org/10.3389/fneur.2022.948830>
26. Federico B, Francesco A, Silvia M et al (2019) Application of diffusion tensor imaging (DTI) and MR-tractography in the evaluation of peripheral nerve tumours: state of the art and review of the literature. *Acta Biomed* 90:68–76. <https://doi.org/10.23750/abm.v90i5-S.8326>
27. Martinez-Heras E, Grussu F, Prados F et al (2021) Diffusion-weighted imaging: recent advances and applications. *Semin Ultrasound CT MR* 42:490–506. <https://doi.org/10.1053/j.sult.2021.07.006>
28. Raya JG (2015) Techniques and applications of in vivo diffusion imaging of articular cartilage. *J Magn Reson Imaging* 41:1487–1504. <https://doi.org/10.1002/jmri.24767>
29. Engelke K, Chaudry O, Gast L et al (2023) Magnetic resonance imaging techniques for the quantitative analysis of skeletal muscle: state of the art. *J Orthop Translat* 42:57–72. <https://doi.org/10.1016/j.jot.2023.07.005>
30. Conti Nibali M, Rossi M, Sciortino T et al (2019) Preoperative surgical planning of glioma: limitations and reliability of fMRI and DTI tractography. *J Neurosurg Sci* 63:127–134. <https://doi.org/10.23736/S0390-5616.18.04597-6>
31. Saupé N, White LM, Stainsby J et al (2009) Diffusion tensor imaging and fiber tractography of skeletal muscle: optimization of B value for imaging at 1.5 T. *AJR Am J Roentgenol* 192:W282–290. <https://doi.org/10.2214/AJR.08.1340>
32. S L-P (2018) Diffusion Tensor Imaging (DTI). *Methods in molecular biology (Clifton, NJ)* 1718. [https://doi.org/10.1007/978-1-4939-7531-0\\_7](https://doi.org/10.1007/978-1-4939-7531-0_7)
33. Barrera CA, Bedoya MA, Delgado J et al (2019) Correlation between diffusion tensor imaging parameters of the distal femoral physis and adjacent metaphysis, and subsequent adolescent growth. *Pediatr Radiol* 49:1192–1200. <https://doi.org/10.1007/s00247-019-04443-z>
34. Bedoya MA, Delgado J, Berman JI et al (2017) Diffusion-tensor imaging of the physes: a possible biomarker for skeletal growth-experience with 151 children. *Radiology* 284:210–218. <https://doi.org/10.1148/radiol.2017160681>
35. Duong P, Mostoufi-Moab S, Raya JG et al (2020) Imaging biomarkers of the physis: cartilage volume on MRI vs. tract volume and length on diffusion tensor imaging. *J Magn Reson Imaging* 52:544–551. <https://doi.org/10.1002/jmri.27076>
36. Melhem ER, Itoh R, Jones L, Barker PB (2000) Diffusion tensor MR imaging of the brain: effect of diffusion weighting on trace and anisotropy measurements. *AJNR Am J Neuroradiol* 21:1813–1820

37. Kvist O, Damberg P, Dou Z et al (2023) Magnetic resonance and diffusion tensor imaging of the adolescent rabbit growth plate of the knee. *Magn Reson Med* 89:331–342. <https://doi.org/10.1002/mrm.29432>
38. Raya JG, Melkus G, Adam-Neumair S et al (2011) Change of diffusion tensor imaging parameters in articular cartilage with progressive proteoglycan extraction. *Invest Radiol* 46:401–409. <https://doi.org/10.1097/RLI.0b013e3182145aa8>
39. de Visser SK, Crawford RW, Pope JM (2008) Structural adaptations in compressed articular cartilage measured by diffusion tensor imaging. *Osteoarthritis Cartilage* 16:83–89. <https://doi.org/10.1016/j.joca.2007.05.013>
40. Bank RA, Bayliss MT, Lafeber FP et al (1998) Ageing and zonal variation in post-translational modification of collagen in normal human articular cartilage. The age-related increase in non-enzymatic glycation affects biomechanical properties of cartilage. *Biochem J* 330(Pt 1):345–351. <https://doi.org/10.1042/bj3300345>
41. Goldman HM, Bromage TG, Thomas CDL, Clement JG (2003) Preferred collagen fiber orientation in the human mid-shaft femur. *Anat Rec A Discov Mol Cell Evol Biol* 272:434–445. <https://doi.org/10.1002/ar.a.10055>

**Publisher's Note** Springer Nature remains neutral with regard to jurisdictional claims in published maps and institutional affiliations.

Springer Nature or its licensor (e.g. a society or other partner) holds exclusive rights to this article under a publishing agreement with the author(s) or other rightsholder(s); author self-archiving of the accepted manuscript version of this article is solely governed by the terms of such publishing agreement and applicable law.

## Authors and Affiliations

Yilu Zhang<sup>1</sup> · Zhuo Cheng<sup>1</sup> · Hailun Peng<sup>1</sup> · Wei Ma<sup>2</sup> · Rui Zhang<sup>1</sup> · Junya Ma<sup>1</sup> · Sijie Gao<sup>1</sup> · Wei Li<sup>1</sup> · Ye Xu<sup>1</sup>

✉ Ye Xu  
yexu@cqmu.edu.cn

<sup>1</sup> Department of Radiology Children's Hospital of Chongqing Medical University, National Clinical Research Center for Child Health and Disorders, Ministry of Education Key Laboratory of Child Development and Disorders, China International Science and Technology Cooperation Base of Child Development and Critical Disorders, Chongqing

Key Laboratory of Pediatric Metabolism and Inflammatory Diseases, 136 Zhongshan Er Lu, Yuzhong District, Chongqing 400000, China

<sup>2</sup> Department of Radiology, The People's Hospital of Yubei District of Chongqing City, Yubei District, Chongqing, China